International Journal of Computer Science and Information Technology
ISSN: 3005-9682 (Print), ISSN: 3005-7140 (Online) | Volume 4, Number 3, Year 2024
DOI: https://doi.org/10.62051/ijcsit.v4n3.14
Journal homepage: https://wepub.org/index.php/IJCSIT/index

Bottle Printing Defect Detection Based on CUDA Accelerated Hybrid Image Registration

Liang Gao [1], Yinghua Liao [2,*], Xingyao Si [3], Qinpeng Luo [1], Jiajun Zhang [1], Lang Wang [1]

[1] School of Mechanical Engineering, Sichuan University of Science and Engineering, Yibin, China

[2] School of Civil Engineering, Sichuan University of Science and Engineering, Yibin, China

[3] YiBin Vocational and Technical College, Yibin, China

ABSTRACT

Objective: in order to detect the printing defects of the legal text of aluminum cans and beer bottles, the difference method after image registration based on difference model is used. Aiming at the problems of insufficient accuracy and slow speed of text image registration, a method of accelerating mixed image registration based on CUDA is proposed. Methods: firstly, rough registration based on speeded-up robust features was used to make the detected image basically coincide with the template image; Secondly, the local deformation fine-tuning based on demons elastic registration algorithm is used to improve the registration accuracy; In order to improve the speed of registration, NVIDIA CUDA architecture is used to accelerate and optimize the algorithm in parallel to complete the registration quickly. The improved hybrid registration method can quickly and accurately complete the registration with the template image. After the differential processing, the artifacts are eliminated by threshold segmentation and morphological corrosion expansion processing to complete the defect detection. Results: the experimental results show that the registration accuracy of this method has been significantly improved, and the CUDA acceleration can achieve about 24 times of the acceleration ratio, which greatly shortens the registration time and meets certain detection requirements. Through the detection of 63 defect samples, the success rate is 98.41%. Conclusion: the hybrid registration scheme proposed in this paper can accurately and efficiently complete the bottle label text registration, and realize the defect detection task, which provides an effective solution for the printing defect detection of the legal text of aluminum cans and beer bottles.

KEYWORDS

Defect detection; Machine vision; Image registration; CUDA parallel acceleration

1. INTRODUCTION

As society progresses, people's quality of life is improving on a daily basis. Consequently, the requirements for product packaging have also become more exacting. Defective packaging can negatively impact the product image, and errors in French printing do not comply with legal requirements. Therefore, the detection of printing defects during production is a crucial step. The ongoing advancement of computer vision and the enhancement of computing capabilities have facilitated the integration of machine vision techniques.

In the field of visual defect detection, the method of image alignment followed by differencing based on a difference model is a frequently utilized approach for defect detection [1-2]. The accuracy and speed of image alignment are of paramount importance in this process. Wang Xing et al [3] employed a SIFT (Scale-Invariant Feature Transform) feature matching-based alignment method to detect defects in printed text on medicine bottles. This method has a faster alignment speed and greater

robustness; however, its alignment accuracy is insufficient for large-area text. Zuo Cai et al [4] utilized a fast Fourier transform method to detect scratches on the surface of printed materials, thereby enabling the detection of defects in printed text. The Fourier transform method is employed to detect the image and align the template image. However, the method is still not sufficiently accurate for complex text image alignment. Hu Fangshang et al [5] addressed the image alignment issue in printing defect detection by They proposed a combination of mathematical morphology, the Hough transform, and the phase correlation principle of the image alignment method. However, this method is unable to achieve accurate alignment in the presence of local aberrations in text images on cylinders or subtle differences.

The current image alignment methods are beset with numerous issues. In pursuit of the research objective, namely the detection of the main body of a substantial number of fine texts, this paper puts forth a hybrid image alignment method. This method employs a two-pronged approach: a primary matching based on feature matching and a secondary alignment method. The former is designed to enhance the accuracy and robustness of the alignment, while the latter is intended to facilitate parallel acceleration through the use of the CUDA architecture [6-7]. This acceleration is necessary to meet the requirements of the defect detection speed.

2. DETECTION OF PRINTING DEFECTS IN FRENCH

The detection method based on image difference involves obtaining two images of the scene and then processing them to eliminate interference. The images are converted to grayscale, filtered, and subjected to other processing steps. After this, the two images are subtracted, and the difference information between them is extracted. This information is then analyzed to identify any defects. In the context of a detection application, the real-time image to be detected is frequently acquired and processed through a process of difference with a standard template. It is important to note that the accuracy and speed of image alignment will have a significant impact on the detection effect. Due to the position of the bottle and environmental vibration, the image to be detected will not be perfectly aligned with the template image, resulting in a certain degree of translation and elastic deformation. This necessitates adjustment to the spatial position through image alignment. Consequently, the accuracy and speed of image alignment represent pivotal considerations in this research. In the detection of printing defects in the French language on wine bottles, there are some displacement deviations in the text portion captured by the camera. Additionally, the text is of a limited quantity, and the curved body of the bottle will also introduce a certain degree of local distortion to the image. Therefore, the alignment accuracy must be higher, the captured image must have a higher resolution, and the image algorithm will require a significant processing time.

In the case of images exhibiting significant displacement transformations, feature point matching-based alignment techniques are frequently employed. Prominent examples include the ORB (oriented fast and rotated brief) algorithm, the scale-invariant feature SIFT algorithm [8], the speeded-up robust features (SURF) algorithm [9], and other feature matching algorithms. Among these, the SURF algorithm has the advantage of stable features, a fast operation speed, and better robustness, which has resulted in its increased usage. When targeting complex elastic local deformation, the common methods are free-form deformation (FFD) alignment based on B-splines, image alignment based on thin plate spline TPS, and Demons image alignment based on optical flow field.

This paper proposes a novel defect detection algorithm based on CUDA-accelerated hybrid image alignment, which is derived from the SURF and Demons algorithms. Firstly, image alignment based on SURF feature matching is employed to establish a coarse correspondence between the image to be detected and the template image, ensuring that their spatial positions are largely aligned. Secondly, the Demons local elasticity-based alignment algorithm is utilized to perform a secondary alignment of text small deformation, thereby enhancing the accuracy. The high resolution of the image results in a slow processing speed for the algorithm. To address this, the NVIDIA CUDA architecture is

employed to enable parallel accelerated computation, thereby enhancing the alignment speed. Subsequently, the difference image between the image to be detected and the template image is obtained through differential processing. Errors are then removed from the image through a series of operations, including threshold segmentation, morphological corrosion expansion processing, and finally, blob analysis is used to establish the location and size of the defects. The basic process is illustrated in Figure 1:

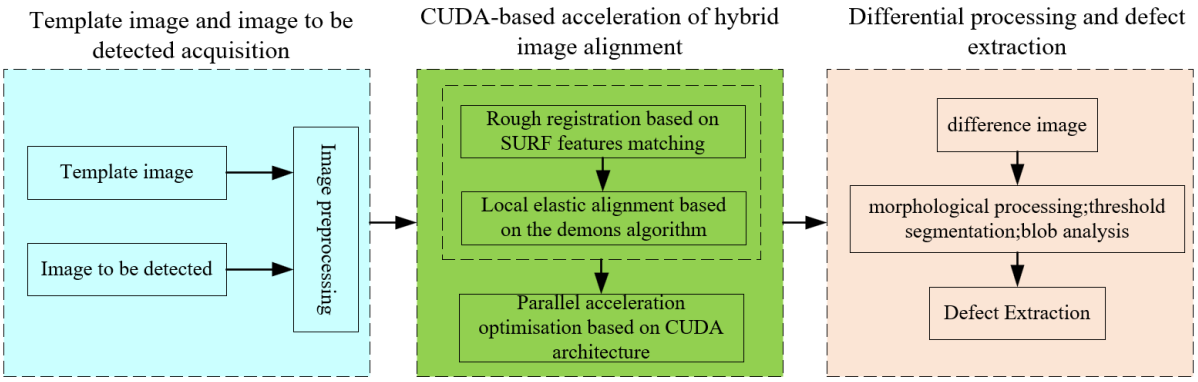

Figure 1. Scheme flow chart

2.1. Image Preprocessing

Machine vision technology is a process that involves the analysis of digital images to detect defects. Therefore, the acquisition of images is of particular importance. The experimental acquisition system for image acquisition is illustrated in Figure 2. In the acquisition of image data, a number of factors, including the surrounding environment, light, and reflections from metal bottles, can contribute to the presence of noise and burrs in the image, rendering it unsuitable for direct detection purposes. Consequently, effective image pre-processing is essential to ensure the reliability of subsequent analysis.

In order to minimize or eliminate the effects of reflections, a coaxial light source is employed to illuminate the object under observation when an industrial camera is utilized for acquisition. The parallel light emitted by a coaxial light source is directed from the side onto a semi-reflector, through which the light is directed onto an object and finally reflected from the object into the lens. The reflected coaxial light is captured by the lens, while the highly reflective diffuse light is rejected, thereby attenuating or eliminating the effect of reflective objects. The schematic diagram is shown in Figure 3:

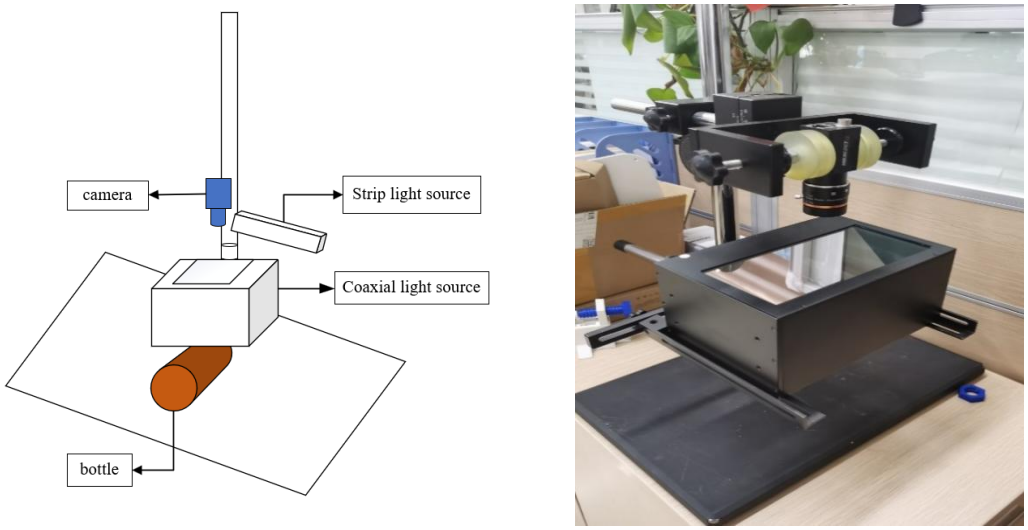

Figure 2. Image acquisition system

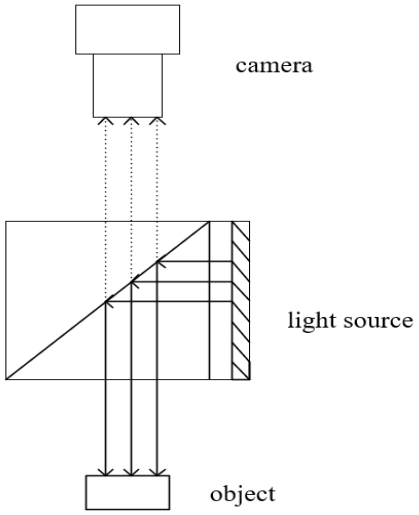

Figure 3. Schematic diagram of coaxial light source

The acquired images are RGB images, which must be clarified and characterized during the image preprocessing stage. This necessitates the implementation of suitable preprocessing methods. Following an empirical evaluation of the available techniques, the image preprocessing steps employed in this study comprise the following sequence: firstly, the image is transformed into grayscale; secondly, binarized segmentation is applied; and thirdly, Gaussian filtering is utilized to remove image noise. A Gaussian filter is a linear smoothing filter that employs a 5×5 convolution kernel for Gaussian convolution of the image. Following processing, the bottle printing image is transformed into a black and white image, wherein the target for detection is separated from the background and the excess background is removed by dividing the region of interest. The printed part to be detected is retained as a template image. The same preprocessing method is also adopted for the image to be detected, and image alignment is subsequently performed. The effect of image preprocessing is demonstrated in Figure 4:

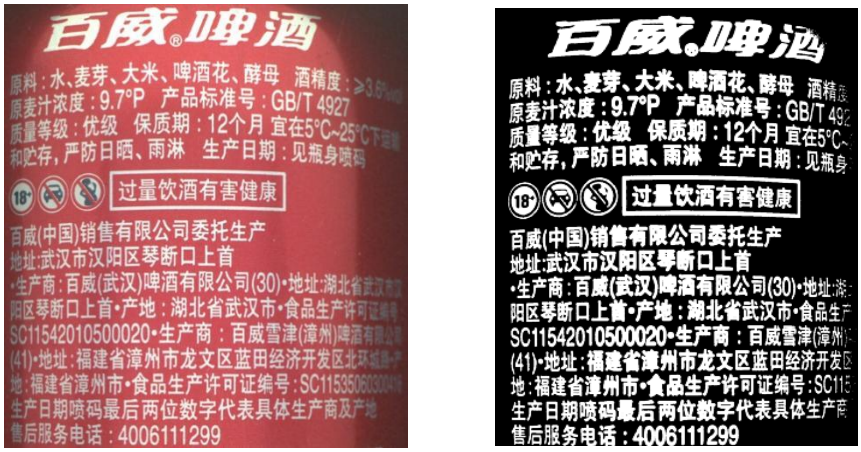

a. Original drawing b. After image preprocessing

Figure 4. Image acquisition and pretreatment

2.2. Coarse Alignment Based on Feature Matching

The most commonly used feature algorithms are ORB, SIFT, SURF, and so forth. Among these, the ORB algorithm is faster, but its accuracy is insufficient. In comparison, the SIFT algorithm has better robustness while maintaining a certain degree of accuracy. As a result, it is employed more extensively in image matching. The SURF algorithm represents an enhancement of the SIFT

algorithm, offering further improvements in matching speed. Consequently, the matching algorithm based on the SURF alignment algorithm is utilized for coarse matching.

The SURF algorithm enhances the extraction and characterization of features through the incorporation of integral images and box filters, thereby markedly enhancing the computational efficiency. The rapid computation of Haar features by integral image (integral image) results in a reduction in the speed of image local rectangle summation operations. In comparison to SIFT, which employs a Gaussian pyramid for feature detection in scale space, SURF introduces the Hessian matrix [10], which is utilized to rapidly convolve the integral image through the use of a box filter, thereby facilitating the more efficient detection of local features. The Hessian matrix is a square matrix comprising second-order partial derivatives of a multivariate function, and the approximate computation of the Hessian matrix enables the rapid identification of the aforementioned matrix. In the context of image analysis, the Hessian matrix is defined as follows (1):

$$H(f(xy)) = \begin{bmatrix} \frac{\partial^2 f}{\partial x^2} & \frac{\partial^2 f}{\partial x \partial y} \\ \frac{\partial^2 f}{\partial x \partial y} & \frac{\partial^2 f}{\partial y^2} \end{bmatrix} \tag{1}$$

The SURF algorithm employs a box filter to execute a convolution operation with the image, effectively transforming the process of image filtering into a problem of adding and subtracting pixel sums between disparate regions within the image. In order to approximate the determinant of the Hessian matrix det(H), it is recommended to use D_{xx}, D_{xy}, and D_{yy} in place of the second-order differentials in the matrix:

$$\det(H) = D_{xx}D_{yy} - (\omega D_{xy})^2 \tag{2}$$

Where: ω is a weighting factor to balance the error due to the use of the box filter approximation, generally taken as 0.9.

The two images to be aligned are first subjected to separate detection of their feature points, which are then matched by the feature matching algorithm. Once the matching points have been identified, the geometric transformation relationship between the two images is calculated using these points. Subsequently, the images are resampled in order to achieve alignment. In contrast to the SIFT algorithm, which employs the gradient histogram descriptor, the SURF algorithm utilises the wavelet descriptor to represent the local structure surrounding the feature points. The wavelet descriptor is more expedient to compute due to its capacity to be calculated efficiently through image integration.

Image coarse matching is conducted via a SURF-based alignment algorithm, which essentially aligns the target image with a significant offset to the template image. This enables the utilization of local elastic alignment, thereby enhancing the accuracy of the process.

2.3. Flexible Alignment Based on Demons Algorithm

The most commonly utilized elastic alignment methodologies are B-spline-based free-form deformation (FFD) alignment, thin plate spline (TPS)-based alignment, and optical flow field-based Demons alignment. B-spline-based FFD deformation entails the distribution of grid points on the image according to a specified spacing, the calculation of the pixel offset for each pixel point in relation to the grid point position, and the subsequent performance of pixel resampling in accordance with the offset. This method is characterized by high accuracy, a wide range of applications, and a high degree of freedom. However, it requires the processing of a substantial amount of data and is associated with a significant computational burden, resulting in prolonged processing times. The thin plate spline (TPS) algorithm necessitates the initial acquisition of multiple pairs of corresponding points within the same regions of the two images. Subsequently, the TPS transform is employed to

calculate the coordinate mapping of each pixel point, ultimately yielding the aligned image. This method exhibits notable advantages, including high accuracy and robust stability. However, it also presents inherent limitations, such as a proclivity for local extreme values and a propensity for extensive computational demands.

The Demons algorithm [11] is a non-rigid image alignment algorithm based on optical flow field theory. It is notable for its reduced computational intensity in comparison to the other two elastic alignment algorithms. The image alignment algorithm in question spreads the pixels of the image to be detected towards the template image, using the gray gradient information of the reference image. This process can be demonstrated through the application of equation (3):

$$u = \frac{(f - m)\nabla m}{|\nabla m|^2} \tag{3}$$

Where: f is the gray scale of the image to be detected and m is the gray scale of the template image.

In their study, H. Wang et al [12] proposed the Active Demons algorithm, which is based on the premise that the forces are mutual. This approach involves incorporating the gradient of the image to be detected into the diffusion force, resulting in a significant enhancement in convergence speed. The underlying equation can be modified as illustrated in (4):

$$u = u_m + u_f = \frac{(f - m)\nabla m}{|\nabla m|^2 + \frac{(f - m)^2}{k^2}} + \frac{(f - m)\nabla f}{|\nabla f|^2 + \frac{(f - m)^2}{k^2}} \tag{4}$$

Where u_m is the forward force of the template image gradient and u_f is the reverse force of the gradient of the image to be detected.

The Demons algorithm employs a coordinate offset calculation based on the gradient of the template image and the difference between the grayscale of the template image and the image to be detected. This is followed by an interpolation and resampling process, whereby the pixels of the image with detection are based on the aforementioned coordinate offsets. The process is then repeated several times until either a pre-defined threshold is reached or a set number of iterations has been completed, with the objective of achieving image alignment. Santos-Ribeiro et al [13] further proposed the Inertial Demons algorithm, which employs a similar approach to that described above. In this case, however, the offset obtained from the previous iteration is added to the next calculation, thereby improving both the convergence speed and the accuracy of the algorithm.

By calculating the coordinate offsets of the template image and the image to be detected, and then repeating this process iteratively, the image to be detected is interpolated and pixel resampled. In the iterative process, the offset of the previous iteration is added to the next calculation, and this process is repeated until a set iteration threshold is reached. During the iteration process, smoothing is performed by Gaussian filtering to ensure that the alignment process is continuous in the global range. The flowchart of the alignment process is shown in Figure 5:

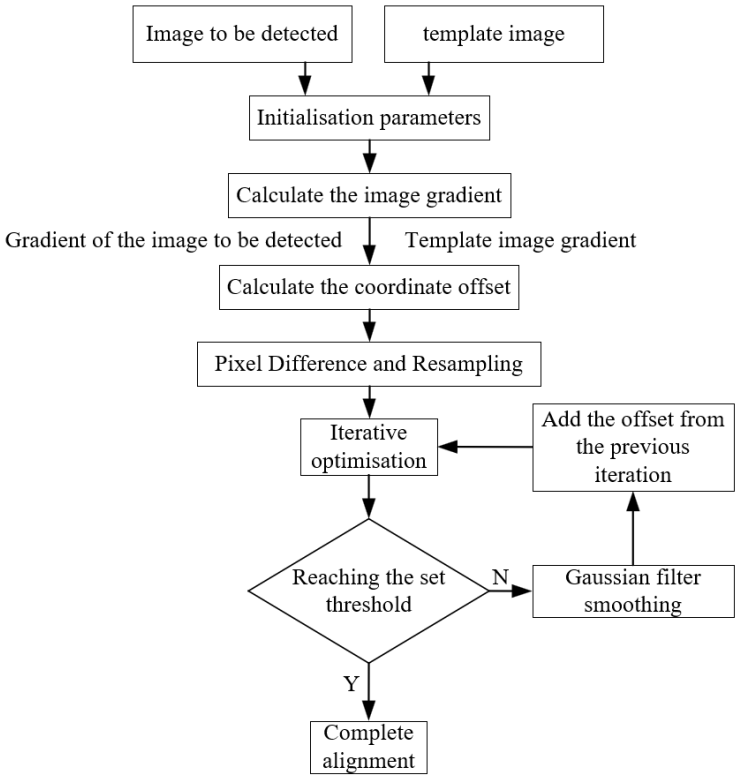

Figure 5. Demons local elastic registration process

After local elastic alignment, the spatial positions of the template image as well as the image to be aligned can be highly corresponding.

2.4. CUDA Parallel Accelerated Alignment

The program runs for an extended period during the elastic alignment process, which is insufficient to meet the industrial inspection requirements. This is due to the necessity of performing pixel calculations on both the floating image and the reference image, as well as the requirement for multiple iterations to achieve image alignment.The CUDA (Compute Unified Device Architecture) framework, introduced by NVIDIA, is a parallel computing framework that utilizes the graphics processing units (GPUs) for general-purpose computing. The framework utilizes a large number of processing units (CUDA cores) in the GPU, which greatly improves the computing speed through parallel computing.

A CUDA program is based on a CPU and GPU heterogeneous platform, where the CPU is the host and the GPU is the device. The main function is executed on the host, while the part that requires acceleration of computation utilizes a kernel function to run on the device. The primary process of a CUDA architecture is as follows: The five steps of the CUDA program are as follows:

(1) Allocation of memory and initialization of data;

(2) Transfer of data from the host to the device;

(3) Calling of the kernel function by the GPU to process the data;

(4) Transfer of data back to the host;

(5) Release of memory.

In order to enhance the computational efficiency of the Demons algorithm, this paper employs the CUDA parallel architecture programming model to divide the original algorithm into three kernel functions for parallel computation, which are designed to address the steps that require a significant

number of operations during the algorithm. The GaussianBlur Kernel is employed for Gaussian smoothing, the Demons Kernel is utilized to implement the repeated iteration component of the computation, and the MovePixels Kernel is used for pixel resampling and interpolation. The computation is accelerated in parallel by the GPU, and the results are transferred back to the CPU after the synchronization thread, which significantly accelerates the computation speed. The primary flow of the parallel acceleration optimization step is illustrated in Figure 6:

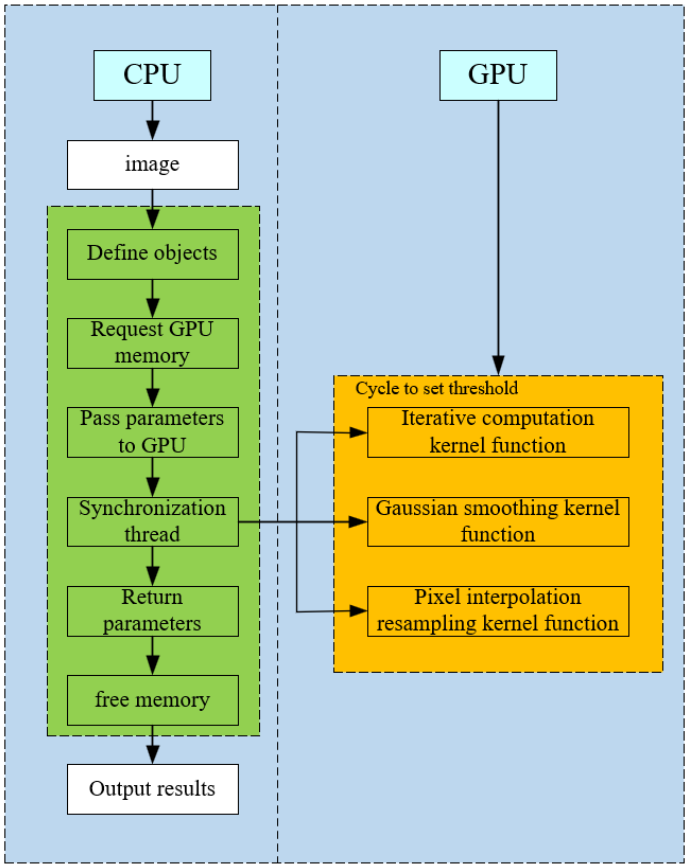

Figure 6. CUDA parallel acceleration

2.5. Differential and Defect Extraction

Following the implementation of coarse alignment and local elastic alignment, the spatial positions of the pixels in the image to be detected and the template image have been significantly overlapped. The method of image difference is then employed to calculate the difference shadows of the two images. Subsequently, the two images are subtracted from each other, thereby highlighting the difference regions in the two images. This process facilitates the extraction of defects. Let us assume that the gray value of the template image is $m(x, y)$, and that the gray value of the floating image is $f(x, y)$. In this case, the expression (5) for calculating the difference is:

$$abs(x, y) = | m(x, y) - f(x, y) | \tag{5}$$

As pixel resampling is conducted concurrently with image alignment, the coordinates within the image are frequently not integers, but rather floating-point numbers. Consequently, an interpolation algorithm is necessary to calculate the pixel value of the floating-point-type coordinate point based on the pixel value of the integer-type points surrounding the floating-point coordinate point, thereby facilitating the resampling process. Consequently, a residual error persists following alignment, and the defect images obtained through differencing frequently exhibit artifacts that impede accurate defect assessment.

To address the issue of artifacts, morphological corrosion expansion processing is employed to remove the residual edges that persist following text differencing, thereby highlighting the defects. Through blob analysis, the location, shape, area size, and other characteristics of the defective target are obtained. Subsequently, based on the predefined grayscale thresholds, the determination of whether a given point constitutes a defect is made. Points that fall below the specified threshold can be disregarded, and finally, the location and characteristics of the defects are ascertained.

3. EXPERIMENTAL RESULTS AND ANALYSIS

In order to ascertain the viability of the proposed methodology, a series of images of Budweiser red aluminium beer bottles in French were collated for experimental validation, with an image resolution of 1280×720. The hardware configuration comprises an Intel(R) Core(TM) i5-12600kf CPU with a processing frequency of 4.5GHz, and the graphics card is an Nvidia Geforce RTX3070 8GB. The software programming environment is a Visio Studio 2022 for Win11 system and CUDA version 11.7. To verify the effectiveness of the algorithm, the images to be detected are aligned with the template image using the SURF feature matching algorithm based on the SURF feature matching algorithm and the hybrid alignment method proposed in this paper, respectively. The defects are then extracted by differential extraction. The alignment effect is evaluated using normalised mutual correlation and other coefficients, and the defect detection effect is investigated. A comparison of the running times of the program before and after acceleration allows the effect of the CUDA parallel acceleration optimisation experiment to be verified.

3.1. Image Alignment and Defect Detection Results

To ascertain the veracity of the image alignment, the evaluation parameters of normalised cross-correlation (NCC) and structural similarity index (SSIM) are employed. NCC represents a methodology for quantifying the similarity between two images, based on the inter-correlation operation in image processing. Normalised cross-correlation (NCC) is a method for measuring the similarity between two images. It is based on the inter-correlation operation in image processing and normalises the inter-correlation result, rendering it insensitive to changes in luminance and contrast. Consequently, it is a commonly used evaluation parameter for image matching effects. The formula for this is given by equation (6).

$$NCC(f,g)=\frac{\sum_{t,j}[f(i,j)-\bar{f}][g(i,j)-\bar{g}]}{\sqrt{\sum_{i,j}[f(i,j)-\bar{f}]^2\cdot\sum_{i,j}g(i,j)-\bar{g}]^2}} \tag{6}$$

In this context, $f(i,j)$ and $g(i,j)$ represent the pixel values of the two images at (i,j), while $\bar{f}$ and $\bar{g}$ denote the average pixel values of the two images, respectively. It should be noted that NCC takes values in the range [-1, 1], with the general understanding that the closer the value is to 1, the higher the degree of similarity between the two images. With regard to SSIM, this measures the similarity between the two images by comparing the similarity between the images in terms of luminance, contrast and structure. It exhibits superior accuracy and robustness in comparison to error measures such as the mean square error.

In this study, the NCC and SSIM metrics are employed as the evaluation criteria for image alignment. The acquired defective sample images are then aligned with the template images. In order to assess the impact of image alignment, three distinct levels of offset images are designated for control testing. The control test is divided into two groups. The first group is image alignment based on SURF feature matching only, while the second group is image alignment using the hybrid alignment method described in this paper. The current production process is highly precise in controlling the orientation of wine bottle labels to a millimetre level, thereby limiting the offset caused by errors during image acquisition. To simulate potential sources of error, three levels of offset x are set up: less than 2 mm,

2 mm to 4 mm, and 4 mm to 6 mm, respectively. The NCC and SSIM values were calculated before and after alignment, and the results were averaged over 10 trials. The results of the SURF feature matching are presented in Table 1. The alignment results are shown in Table 1.

Table 1. Surf registration effect

Offset/(mm)	NCC		SSIM	
	Before registration	After registration	Before registration	After registration
$0 \le x < 2$	0.938	0.974	0.870	0.948
$2 \le x < 4$	0.796	0.956	0.852	0.932
$4 \le x < 6$	0.688	0.938	0.849	0.910

The mixed registration effect results are shown in Table 2:

Table 2. Mixed registration effect

offset/(mm)	NCC		SSIM	
	Before registration	After registration	Before registration	After registration
$0 \le x < 2$	0.938	0.984	0.870	0.986
$2 \le x < 4$	0.796	0.972	0.852	0.956
$4 \le x < 6$	0.688	0.954	0.849	0.952

As evidenced by the above table, the current hybrid alignment method has enhanced alignment precision, facilitates the elimination of a greater number of differential artefacts resulting from alignment inaccuracies, and enables the more effective extraction of defects.

Following the processing of the two images after alignment, the difference image will be subjected to threshold segmentation, morphological corrosion expansion in order to eliminate the artefacts, and finally, the location and size characteristics of the defects will be extracted through blob analysis. This will complete the defect detection process. The effect diagrams of image differencing, processing and defect detection are presented in Figure 7 and 8:

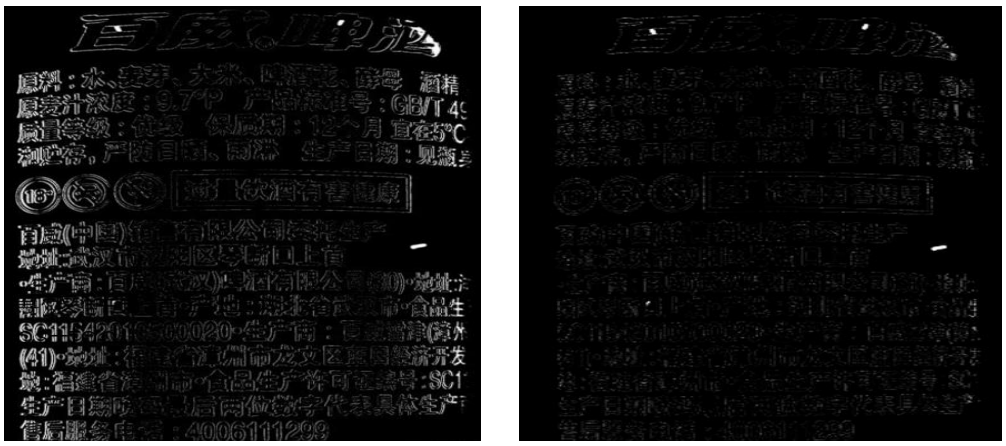

a. Direct feature matching image registration difference map; b. Mixed registration difference graph

Figure 7. Image difference effect comparison

a. Printing defects 1 b. Printing defects 2 c. Printing defects 3 d. Printing defects 4

Figure 8. Defect detection effect

As illustrated in Figure 7, a and b, the hybrid alignment method proposed in this paper demonstrates a notable enhancement in alignment precision. The differenced image effectively mitigates the impact of alignment errors, which otherwise introduce text edge artefacts. Consequently, subsequent image processing can more accurately extract defective features, thereby validating the progressive efficacy of the hybrid alignment method proposed in this study. Ultimately, 63 instances of defective samples were identified, resulting in a success rate of 96.82%.

3.2. CUDA Parallel Acceleration Results

The process of image alignment necessitates the calculation of all pixel points within the image, which results in a significant reduction in processing speed, particularly when working with high-resolution images. For instance, the time required for the processing of a 4096×3000 image exceeds 50 seconds. Similarly, the utilisation of 1280×720 images necessitates a processing time of over 19 seconds, which is inadequate for meeting the demands of actual production. Consequently, there is a necessity for optimisation and acceleration of the process. In order to verify the effect of CUDA parallel acceleration, the experiment counted the total elapsed time and acceleration ratio of the two operations before and after the parallel acceleration of multiple groups. Each group of experiments took the average of 10 running times, and the results are shown in Tab 3. As evidenced by the data in the table, the parallel acceleration effect can achieve approximately 24 times the acceleration ratio, and the alignment time is reduced from an average of 19.216 seconds to an average of 0.785 seconds. This significantly reduces the alignment time, thereby meeting the detection speed requirements.

4. CONCLUSIONS

This paper proposes a method for detecting defects in the printing of wine bottles. The method is based on CUDA-accelerated hybrid image alignment difference. This approach achieves a high degree of correspondence between the spatial position of the image to be detected and the template image. This is achieved through hybrid image alignment based on coarse alignment of SURF feature matching combined with local elasticity alignment based on the Demons algorithm. Furthermore, the method makes use of the parallel acceleration optimisation of the CUDA architecture. This improves the algorithm's performance. The discrepancy between the aligned image and the template image can be processed through threshold segmentation, morphological processing and blob analysis, which can facilitate the detection of defects in French printing on wine bottles. The experimental results allow the following conclusions to be drawn:

The hybrid alignment scheme markedly enhances alignment precision, substantially diminishes differential artefacts resulting from alignment inaccuracies, and is capable of discerning defect characteristics through processing, thereby facilitating the completion of the defect detection process.

The time required for alignment is significantly reduced by CUDA parallel optimisation, enabling the inspection task to be completed in a shorter time frame and thus meeting certain defect detection requirements.

Subsequent research will entail more comprehensive investigations into the precision and velocity of image alignment, with the objective of further enhancing the efficiency of defect detection while concurrently augmenting accuracy to align with the escalating requirements of factory production.

REFERENCES

[1] LI B Y, YANG W H, YANG L, et al. Research on printing defect detection of fertilizer packaging based on template matching [J]. Printing and Digital Media Technology Study, 2023, (02): 39-49. DOI: 10.19370/j.cnki.cn10-1886/ts.2023.02.005

[2] ZHANG D H, ZHU Z F, LI Y Q et al. Research progress of two dimensional image quality defect detection based on machine vision [J]. Packaging Engineering, 2023, 44(23): 198-207. DOI:10.19554/j.cnki.1001-3563.2023.23.024.

[3] WANG X, LIU Z Y, SONG X L et al. Printed Word Defect Detection of Medicinal Glass Bottle Based on the Image Registration [j]. Packaging engineering, 2017, 38 (21): 180-185. DOI:10.19554/j.cnki.1001-3563.2017.21.037.

[4] ZUO C, ZHANG Y B, QI Y S, et al. Detection of surface scratch defects of printing products based on machine vision [j]. Printing and Digital Media Technology Study, 2023, (05): 42-48. DOI:10.19370/j.cnki.cn10-1886/ts.2023.05.004.

[5] HU F S, GUO H, XING J P, et al. Image registration based on label printing defect detection [j]. Optical Technique, 2017, 43 (01): 16-21. DOI:10.13741/j.cnki.11-1879/o4.2017.01.004.

[6] NIU T, LIU L D, WU Y H. Image registration algorithm based on CUDA acceleration [J]. Computer Systems & Applications, 2023, 32(01): 146-155. DOI: 10.15888/j.cnki.csa.008889.

[7] ZHOU L J, XIAO S D, LI S Y, et al. Accelerating digital image processing based on SURF and GPU [J]. Transducer and Microsystem Technologies, 2022, 41(03): 98-100. DOI:10.13873/J.1000-9787(2022)03-0098-03.

[8] GAO S, YUAN X P, GAN S, HU L, BI R, LI R B, LUO W D. UAV image matching method integrating SIFT algorithm and detection model optimization [J]. Spectroscopy and Spectral Analysis, 2022, 42(05):1497-1503.

[9] WU Y Q, WANG Z L. Remote sensing image registration algorithm based on improved surf in wavelet domain [J]. Journal of Tianjin University (Science and Technology), 2017, 50(10): 1084-1092.

[10] GAO Z Z, WEI B, PAN Z K, et al. Image dehazing based on dark channel prior and Hessian regularization [J]. Journal of Graphics, 2020, 41(01):73-80.

[11] ZHANG D, HUANG H, SHANG Z H. Active demons non-rigid image registration algorithm based on mutual information [J]. Laser & Optoelectronics Progress, 2020, 57(16):124-130.

[12] ZHENG W ZHOU Y, LI W H, et al. Research on DTI multi-channel registration based on variable inertia coefficient active demons algorithm [J]. Journal of Hebei University (Natural Science Edition), 2021, 41(04):436-442.

[13] SANTOS-RIBEIOR A, NUTT D J, McGONIGLE J. Inertial demons: a momentum-based diffeomorphic registration framework [C]. Medical Image Computing and Computer-Assisted Intervention-MICCAI 2016: 19th International Conference, Athens, Greece, October 17-21, 2016, Proceedings, Part III 19. Springer International Publishing, 2016: 37-45.